E-ISSN: 2829-7687
Journal of Fibers and Polymer Composites
Vol. 5 No. 1 (2026): 71-86

The Effect of Temperature on Manufacturing Process of Tannin Acid-Based Adhesive Materials on Mechanical and Physical Properties

Mastariyanto Perdana [a, b], Hairul Abral [a, c *], Lovely Son [a], Nanang Masruchin [d], Muhammad Azmi [b], Kadriadi [a, e]

[a] Department of Mechanical Engineering, Universitas Andalas, Padang, Indonesia,
[b] Department of Mechanical Engineering, Institut Teknologi Padang, Padang, Indonesia
[c] Laboratory of Nanoscience and Technology, Department of Mechanical Engineering, Universitas Andalas, Padang, Indonesia
[d] Research Center for Biomass and Bioproducts, National Research and Innovation Agency of Indonesia (BRIN), Cibinong, Indonesia
[e] Department of Mechanical Maintenance Engineering, Politeknik Industri Logam Morowali, Morowali, Indonesia

Abstract. *This study focuses on the development and characterization of adhesives based on Polyvinyl Alcohol (PVA), Tannic Acid (TA), and Cellulose Nanofibre (CNF). The main objective is to optimize the temperature used in the production process. Phenol-formaldehyde and other synthetic adhesives frequently encounter environmental obstacles, necessitating the search for more ecologically sound alternatives. TA, a naturally occurring polyphenolic molecule, has significant potential as an eco-friendly glue ingredient. This study assesses the impact of temperature fluctuations (30, 45, 60, 75, and 90°C) during the glue manufacturing process on its mechanical characteristics, specifically emphasizing shear stress. Experiments were conducted at a rotational speed of 1500 revolutions per minute (RPM) for 30 minutes. The results indicated that the adhesive performed best at 90°C, achieving a maximum shear stress value of 3.41 MPa. The results demonstrated a significant enhancement in the shear strength of the bioadhesive, exhibiting an approximately sixfold increase as the processing temperature was elevated from 30°C to 90°C. Microstructural analysis reveals that the voids formed during the mixing process decrease at this specific temperature. The results indicate that elevated temperatures lead to a significant reduction in void formation. The FTIR measurement revealed the absorption of hydroxyl groups around 3305 cm^{-1}, suggesting the presence of robust crosslinking. Furthermore, elevated temperatures lead to a significant reduction of free OH- groups within the bioadhesive. The PVA/TA/CNF adhesive possesses extensive potential for application in industries that necessitate adhesives with exceptional strength. The study is anticipated to offer comprehensive understanding of how to improve the manufacturing process of TA-based adhesives, and its impact on the creation of adhesive materials that are more sustainable and environmentally friendly.*
Keywords: *polyvinyl Alcohol; tannic acid; cellulose nanofibre; adhesive properties; mechanical properties.*

1. Introduction

Adhesives are essential in many industries, particularly in the manufacture of wood composites. However, synthetic adhesives such as phenol-formaldehyde, urea-formaldehyde, and melamine formaldehyde often pose environmental concerns, including the release of harmful

https://doi.org/10.55043/jfpc.v5i1.570
Received February 8, 2026; Received in revised form March 5, 2026; Accepted March 15, 2026; Published March 30, 2026
* First corresponding author
Email: abral@eng.unand.ac.id

formaldehyde [1,2]. Consequently, the search for more environmentally friendly alternatives is urgently needed. Tannic Acid (TA), a natural polyphenolic compound extracted from plants and possessing remarkable adhesive properties, has great potential to serve as an environmentally friendly adhesive material [3]. The adhesive properties of TA stem from the ability of its hydroxyl phenolic groups to participate in various non-covalent interactions, which enable them to form strong bonds with various substrates, both rigid and flexible [4,5].

Previous studies have investigated the use of TA in the manufacture of bio-based adhesives and shown that it can be used for various purposes, such as underwater adhesives and water resistance [6,7]. The antimicrobial properties of TA can also stop bacterial growth and biofilm formation, increasing its value for the adhesive industry [8,9]. Tannic acid (TA) exhibits antimicrobial and anti-biofilm activity primarily due to its polyphenolic structure, which enables multiple mechanisms of microbial inhibition. TA acts as a protein-precipitating agent, binding to bacterial surface proteins and membrane components through hydrogen bonding and hydrophobic interactions, thereby increasing membrane permeability and inducing cellular leakage [10–12].

The molecular interaction of TA with polymer matrices and substrates has also been studied. This research demonstrates TA's ability to promote strong adhesives and cross-linking properties that result in high-strength adhesive bonds [13,14]. However, there are still issues in achieving ideal mechanical properties without synthetic cross-linkers [15]. This study also shows that process parameters such as temperature and curing conditions can affect the performance of TA-based adhesives; however, further research is needed to understand the specific effects of temperature changes on shear stress and other mechanical characteristics. Studies on tannic-acid-based adhesives demonstrate that curing temperature and conditions strongly affect adhesive bonding strength and mechanical properties, showing that optimal temperature ranges must be identified for improved performance [16]. In bio-epoxy adhesive systems incorporating tannic acid and other polyphenolic components, higher curing temperatures and pressures were shown to improve tensile shear strength, suggesting that processing temperature and curing conditions influence crosslink density and adhesive performance [17]. The increase in processing temperature significantly influenced the intermolecular interactions and microstructural evolution of the bioadhesive. Elevated temperatures enhanced molecular mobility, promoting more effective hydrogen bonding between functional groups while simultaneously reducing viscosity, which improved chain diffusion and interfacial contact. This condition facilitated a more homogeneous matrix and minimized void formation during curing, thereby contributing to improved mechanical performance.

The incorporation of cellulose nanofibers (CNF) played a crucial role as both a reinforcing agent and a network stabilizer. Owing to their high aspect ratio and abundant hydroxyl groups,

CNF promoted additional hydrogen bonding interactions and stress transfer within the matrix, resulting in a more compact, stable, and mechanically robust adhesive structure.

This study aims to assess the impact of temperature fluctuations on the mechanical characteristics of adhesives made from TA during the production process. Unlike previous studies focusing on formulation composition or mixing time, the present work systematically elucidates the role of processing temperature on microstructural evolution and shear performance of PVA/TA/CNF adhesives, thereby establishing a direct processing–structure–property relationship. The main emphasis of this study is on shear stress analysis. Experiments were conducted at different temperatures (30, 45, 60, 75, and 90°C) using a consistent mixing rate of 1500 RPM for 30 minutes. Additional characterization techniques, including Fourier Transform Infrared Spectroscopy (FTIR), Digital Microscope (DM), and Scanning Electron Microscopy (SEM), were used to analysis the chemical structure and surface morphology of the adhesive. This study aims to provide a comprehensive understanding of how to optimize the TA-based adhesive manufacturing process and its impact on the advancement of more sustainable and environmentally friendly adhesive materials.

2. Materials and Methods

2.1. Materials

This study used TA powder (20 g), which is a 100% extract of Uncaria Gambier (UG) obtained from CV. Kempan Sumatera Resource, now the Uncaria Gambier Innovation Centre, Lima Puluh Kota, West Sumatra, Indonesia. Additionally, liquid PVA (79 g) with a freezing point of < -10 °C from PT. Asia Duta Mulya, DKI Jakarta, Indonesia, and CNF (1 g) from Nanografi Nano Technology, Çankaya/Ankara, Turkey, were also used. This study specifically investigates a single compositional ratio of the constituent materials in the bioadhesive, with the primary focus placed on evaluating its performance across various processing temperatures.

2.2. Preparation of TA Powder

The preparation of TA powder (20 g) began with a grinding process using a mortar and pestle. The resulting powder was then sieved through a 400 mesh to obtain particles measuring 37µ. The prepared TA powder was then transferred to a mixing container. The mixing process with other materials is carried out using a hand mixer at a speed of 1500 RPM for 30 minutes to ensure the homogeneity of the mixture. Rotation and mixing time variable were selected based on previous optimization results to ensure homogeneous dispersion [18]. Temperature control was applied externally during processing. Schematic of PVA/TA/CNF adhesive manufacturing and testing as shown simply in Fig. 1.

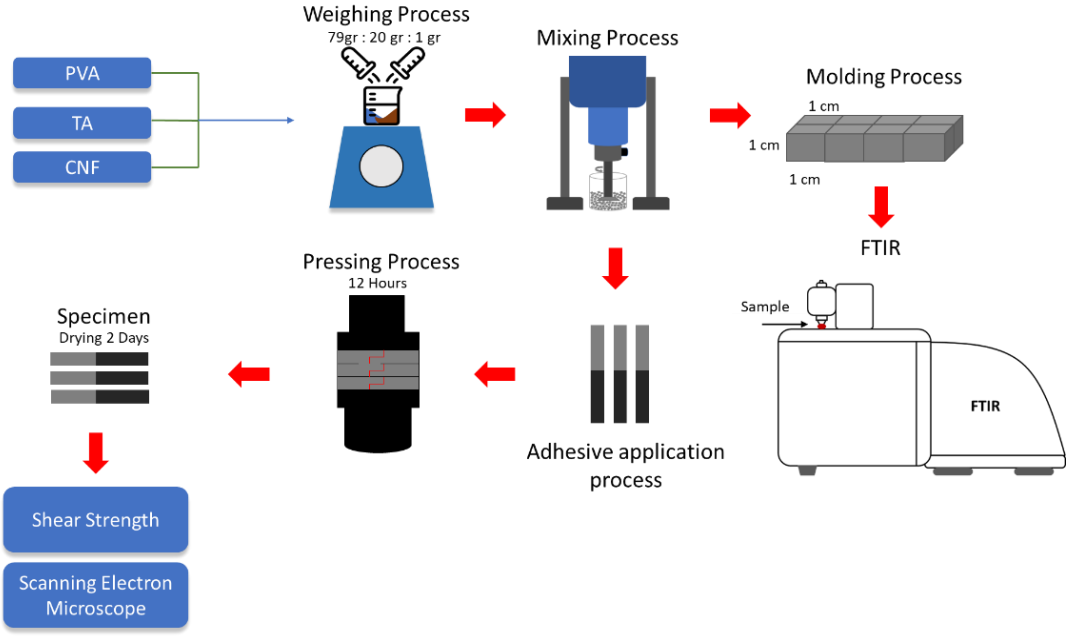

Fig. 1. Schematic of PVA/TA/CNF adhesive manufacturing and testing

2.3. Test Specimen Preparation

This study utilized four testing methods: shear stress testing, microstructure inspection using a digital microscope and Scanning Electron Microscopy (SEM), and Fourier Transform Infrared Spectroscopy (FTIR) analysis. The procedure for preparing specimens/substrates for shear stress testing includes measuring dimensions in accordance with ASTM D-1002 criteria and fabricating jigs for testing purposes using a universal machine. The process of preparing specimens for microstructure observation and FTIR testing includes printing and drying specimens measuring 10 mm x 10 mm x 10 mm.

2.4. Shear Strength Testing

Shear strength testing was conducted on metals in accordance with ASTM D-1002 standard [19]. Each sample was pressed for 24 hours and dried for 2 days. Shear stress testing was conducted at room temperature using a Universal Testing Machine (UTM). Shear testing was conducted six times for each sample variation.

2.5. Digital Microscope (DM) Observation

Microstructural observations were performed on all test materials. The microstructure was studied using a digital microscope with 1000x magnification. The purpose of this observation was to visually detect and identify agglomeration or clustering in TA powder after combining it with other materials. Each sample variation was observed using DM.

2.6. Scanning Electron Microscope (SEM) observation

The surface morphology of the material was observed at high magnification using Scanning Electron Microscopy (SEM), which provides a more comprehensive observation than using DM.

SEM testing began with the preparation of a 10 mm x 10 mm x 10 mm sample. Next, the sample underwent a gold coating procedure, after which the sample structure was observed.

2.7. Fourier Transform Infrared Spectroscopy (FTIR) Analysis

Fourier Transformed Infrared Spectroscopy (FTIR) testing is performed to detect functional groups, identify chemicals, and analyse sample mixtures non-destructively. The infrared portion of the electromagnetic spectrum covers wavelengths ranging from 14,000 $cm^{-1}$to 10 cm^{-1}. The infrared region is categorised into three segments based on these wavelengths: Near infrared (14000-4000 cm^{-1}) is sensitive to overtone vibrations. Mid-infrared (4000-400 cm^{-1}) is associated with molecular vibrational energy transitions and provides information about functional groups. Far-infrared (400-10 cm^{-1}) is used to analyse molecules with heavy atoms, such as inorganic compounds, although it requires special techniques. Compounds are often analysed in the mid-infrared (IR) region [20]. Each specimen in this investigation produced an FTIR spectrum using a PerkinElmer Frontier C90704 Spectrum IR Version 10.6.1 instrument. This equipment is an ATR-FTIR spectrometer capable of performing in-situ analysis on samples. The duration of this testing procedure is approximately 5 to 7 minutes per sample in a single test.

3. Results and Discussion

3.1 Shear Stress

Table 1 shows the shear testing results of bioadhesive A graph of the shear stress test results was obtained as shown in Fig. 2 to see the increase in stress based on 5 temperature variations.

Table 1. Shear stress test results for adhesive materials

Temperature (°C)	Average Force (N)	Shear Stress (MPa)
30	153.69	0.48 ± 0.11
45	353.16	1.11 ± 0.27
60	327.00	1.03 ± 0.04
75	1043.13	3.29 ± 0.24
90	1082.37	3.41 ± 0.27

Shear stress refers to the stress applied in a direction parallel to the surface of the object [21]. The shear test results, as shown in Fig. 2, indicate that the shear stress value increases significantly with increasing temperature. The highest shear stress value of 3.41±0.27 MPa was observed at a temperature variation of 90°C. At 30°C, the relationship between temperature and shear stress is characterized by low values, resulting in a shear stress value of 0.48 ± 0.11 MPa. However, at 45°C, the shear stress value increases to 1.11±0.27 MPa. Nevertheless, the shear stress value decreased to 1.03±0.04 MPa when the test temperature was set at 60°C.

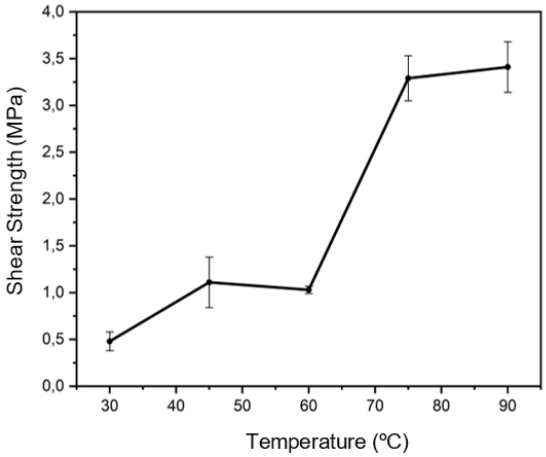

Fig. 2. Shear stress test values for PVA/TA/CNF adhesive

The decrease in shear strength observed at 60 °C may be attributed to a transitional structural state of the adhesive network. At this intermediate temperature, partial disruption of initial hydrogen bonds can occur due to increased thermal energy, while the reformation and stabilization of stronger intermolecular interactions have not yet been fully established. In terms of data variability, the higher standard deviation at 45 °C indicates broader dispersion and reduced uniformity, suggesting greater uncertainty in the mean values. Conversely, the smaller standard deviation at 60 °C reflects more consistent and representative data. Consequently, the observed reduction in shear strength at 60 °C likely falls within the range of experimental deviation and may not signify a substantial decline in material performance**.** The presence of several voids in the adhesive specimens tested on the substrate was clearly visible in the microstructural findings shown in Fig. 3(c) and Fig. 4(c). At test temperatures of 75°C and 90°C, there was a significant increase in shear stress values to 3.29±0.24 MPa and 3.41±0.27 MPa, respectively. By analyzing the graph depicted in Fig. 2, it can be determined that the optimal temperature for the TA adhesive manufacturing process is 90°C. Previous studies have shown that the optimal mixing time for a PVA/TA/CNF-based bioadhesive, prepared at a mixing temperature of 30 °C and a mixing speed of 1500 rpm, resulted in a shear strength of 3.47 MPa [18]. The increase in processing temperature during the fabrication of PVA/TA/CNF bioadhesives contributes to improved shear strength, indicating more effective intermolecular interactions.

3.2 Digital Microscope (DM)

Observation of the microstructure of the adhesive at various temperatures using a DM with 1000x magnification showed significant variations in material characteristics. This can be seen in Fig. 3.

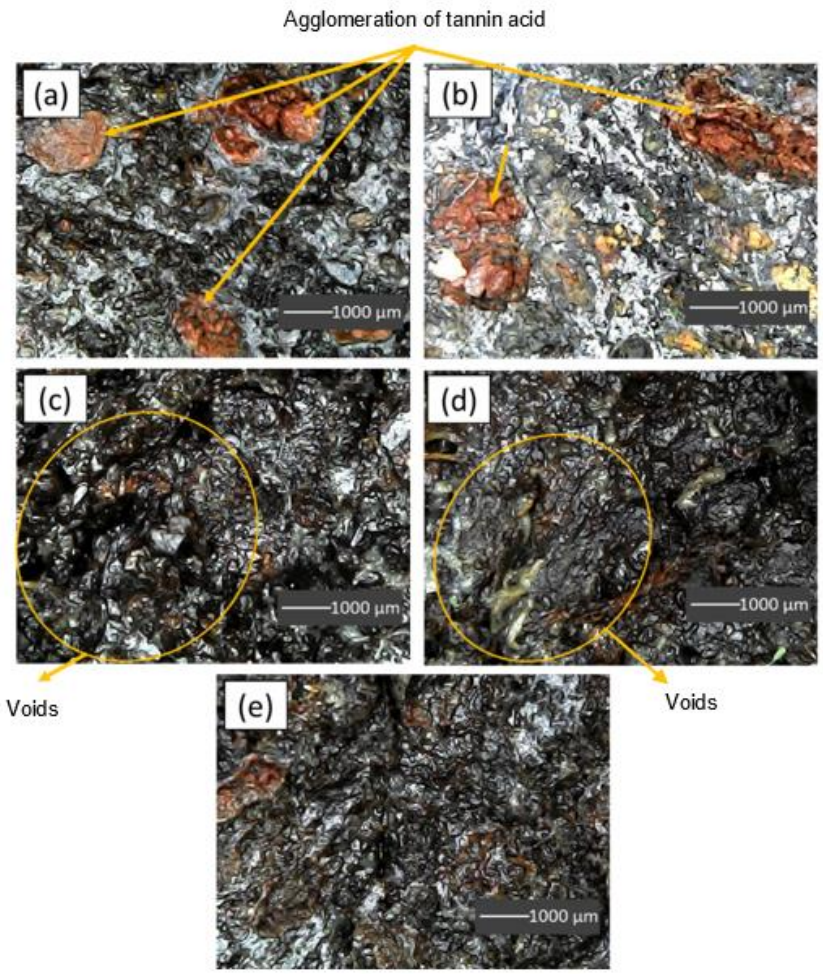

Fig. 3. Observation of the microstructure of PVA/TA/CNF adhesive using DM, (a) Temperature 30 °C; (b) Temperature 45 °C; (c) Temperature 60 °C; (d) Temperature 75 °C; and (e) Temperature 90 °C.

Fig. 3(a) and (b) show that reveal non-uniform distribution and agglomeration of tannic acid, with aggregate sizes visually estimated between $\pm$200–800 µm. The presence of these large agglomerates indicates suboptimal dispersion, which may compromise the structural uniformity of the matrix.

Fig. 3(c) and (d) highlight voids with diameters ranging from ±100 to 500 µm, as estimated against the 1000 µm scale bar. These features are classified as macroporosity, which typically encompasses pores exceeding 100 µm, as opposed to microporosity (<10 µm) and mesoporosity (10–100 µm). The dominance of macropores within the bioadhesive system suggests the presence of air entrapped during the mixing and curing stages.

In contrast, Fig. 3(e) reveals a more compact surface morphology with a relatively uniform phase distribution and minimal visual evidence of large agglomerates or macro-voids. This indicates enhanced macro-homogeneity, likely resulting from a more effective mixing process that suppressed component segregation and large pore formation. After reaching a temperature of 90°C, microscopic examination shows no voids in the adhesive material. The uniform

microstructure without empty voids contributes to the maximum shear stress value obtained at this temperature. These findings indicate that a temperature of 90°C is the most optimal setting for the production of the adhesive under investigation.

3.3 Scanning Electron Microscopy (SEM)

SEM enables the observation of microstructures at the micro scale to provide a more detailed picture of the microstructure of adhesive materials at various temperatures. This allows for the visualization of morphology and surface structure at the micro scale, which provides an understanding of the adhesion mechanism and properties of bio-based adhesives [22,23]. Fig. 4 shows the results of microstructural observation using SEM. Using SEM, the surface topography and morphology of the adhesive interface can be assessed in detail. This technique allows for an explanation of the adhesion mechanism and identification of areas with potential for improvement to increase shear strength [22,24].

Based on direct comparison with the scale reference, the regions indicated as tannic acid agglomerations in Fig. 4(a) and (b) exhibit characteristic dimensions in the range of approximately 2–8 µm. These micrometer-scale secondary phase domains suggest that the dispersion of tannic acid within the polymer matrix is not fully uniform. Agglomerates larger than ~5 µm may act as local stress concentration sites, potentially influencing the mechanical response of the bioadhesive.

In Fig. 4(c) and (d), the observed voids present estimated diameters of approximately 1–5 µm. According to pore size classification based on dimensional scale, pores smaller than 2 µm can be categorized as fine microporosity, whereas pores within the 2–10 µm range fall into the lower mesoporosity regime. Therefore, the bioadhesive structure under these conditions is predominantly characterized by microporosity to low mesoporosity. Such pores are likely associated with entrapped moisture, solvent evaporation, or incomplete consolidation during the curing process.

In contrast, Fig. 4(e) shows a more continuous and compact matrix morphology, with a relatively uniform phase distribution and a reduced frequency of detectable voids. Semi-quantitative observation indicates the absence of dominant pores larger than approximately 3 µm, reflecting a more controlled porosity level and improved microstructural homogeneity. This structural refinement provides a more objective basis for correlating microstructural features with the mechanical performance of the bioadhesive. The presence of voids can affect the mechanical performance of materials, such as a decrease in strength, stiffness, and durability. Some mechanical properties of polymer matrix composites that are greatly affected by voids are flexural performance, impact resistance, tensile properties, and a decrease in interlaminar shear strength [25–27].

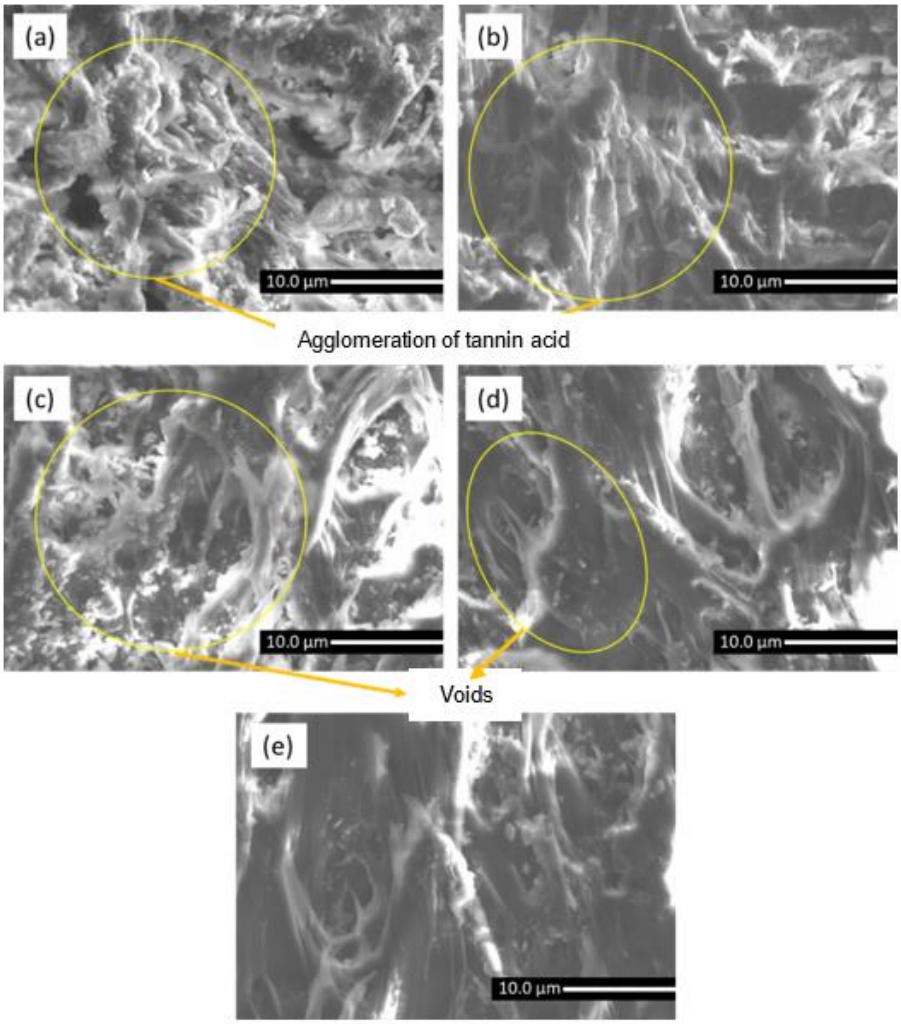

Fig. 4. Observation of the microstructure of the adhesive using SEM, (a) Temperature 30 °C; (b) Temperature 45 °C; (c) Temperature 60 °C; (d) Temperature 75 °C; and (e) Temperature 90 °C

SEM observations show that these voids are randomly distributed throughout the material, creating areas of high stress concentration. Then, at a temperature of 75°C, the number of voids appears to decrease and shows a more uniform distribution with fewer voids, which contributes to an increase in shear stress values. SEM observations reveal that this reduction in voids is related to an increase in material homogeneity. Then, at the highest temperature tested in this study, namely 90 °C, microstructural observations with SEM show the disappearance of voids in the adhesive material. This homogeneous microstructure free of voids contributed to the highest shear stress value achieved, which was 3.41±0.27 MPa. SEM observations at this temperature also showed an increase in interparticle bonding, which contributed to an increase in material strength.

3.4. Fourier Transform Infrared Spectroscopy (FTIR)

Table 2 displays the wave absorption results obtained from the adhesive, categorised based on effect of temperature.

Table 2. ATR-FTIR wave absorption of PVA/TA/CNF adhesive

Temperature (°C)	Hydroxyl (-OH) Absorption (cm^{-1})	Average absorption wavelength (cm^{-1})
PVA	3269	3580–3000
30	3269	3580-3000
45	3298	3465-3206
60	3303	3455-3005
75	3299	3460-3151
90	3305	3489-3011

FTIR analysis is used to identify chemical changes in adhesives at various temperatures. Through FTIR analysis, changes in intensity and peak position associated with hydroxyl functional groups can be observed. The FTIR analysis provides indirect evidence of molecular interactions within the bioadhesive. This can be seen through the FTIR spectra in Fig. 5.

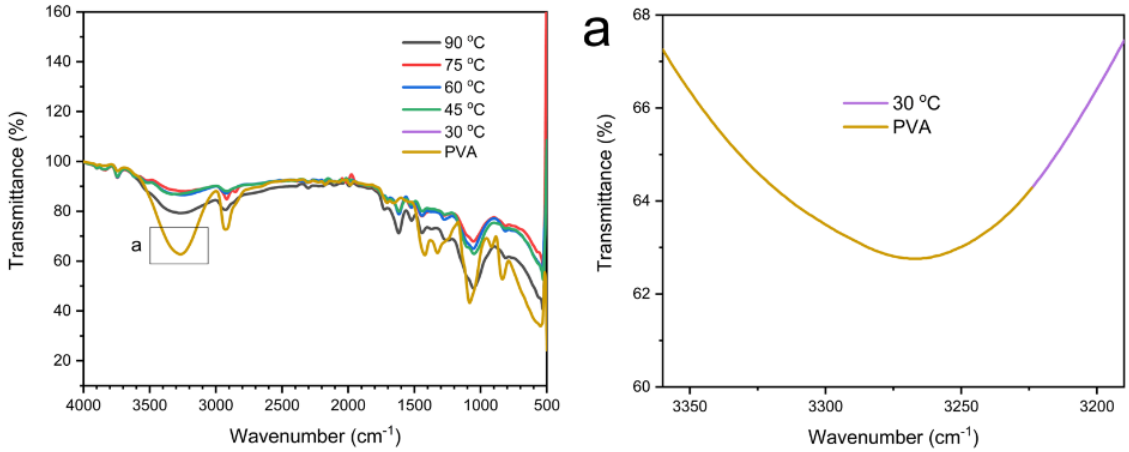

Fig. 5. ATR-FTIR spectra of PVA/TA/CNF adhesives at varying temperatures (a) Pure PVA and PVA/TA/CNF at 30 °C

Based on the FTIR spectra in Fig. 5, the spectrophotometer data illustrates the diversity of functional groups that form compounds in PVA/TA/CNF adhesives. These functional groups play a crucial role in directing the chemical reaction of PVA/TA/CNF during the polymerization process that transforms it into an adhesive material. The stretching that occurs at the hydroxyl group (-OH) value is very far, as seen in the average wavelength range of 3500-3000 cm^{-1}, which is also presented in Table 2. In addition, PVA and the mixture at a temperature of 30 ºC have the same value, as visualized in Fig. 5(a). In the 2000–500 cm^{-1} region, the spectra indicate that temperature primarily modulates the intensity and sharpness of absorption bands associated with C=O, C–O, and C–O–C functional groups, without altering the fundamental chemical structure of the PVA/TA/CNF system. The absence of new characteristic peaks further confirms that no additional covalent bond formation occurs within this temperature range.

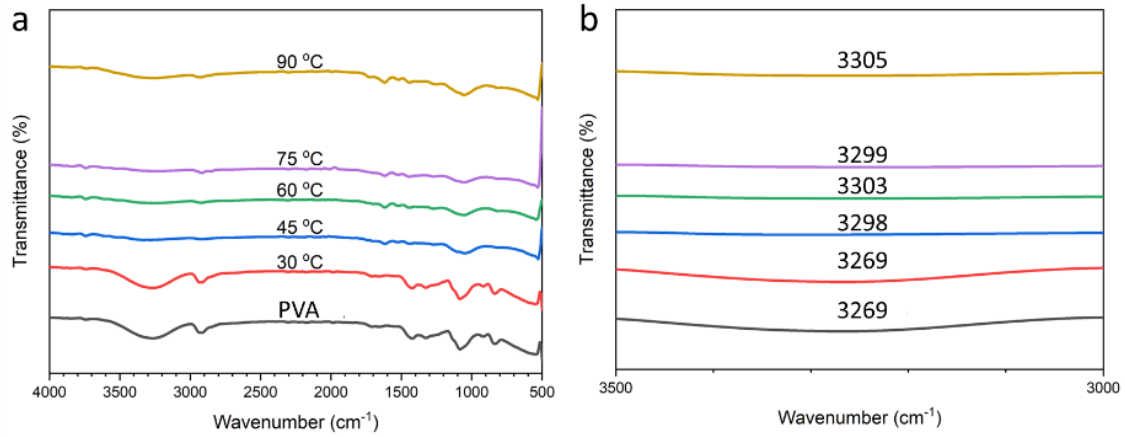

Fig. 6. (a) ATR-FTIR spectra of PVA/TA/CNF adhesive (b) hydroxyl groups of PVA/TA/CNF 3500-3000 cm^{-1}

Based on Fig. 6, the hydroxyl group of PVA/TA/CNF adhesive with a mixing temperature variation of 30 °C shows an absorption value at 3269 cm^{-1} with an average absorption wavelength of 3500-3000 cm^{-1}. This value is consistent with the ATR-FTIR analysis results for PVA without mixing, as presented in Fig. 5(a) and Fig. 6(a). At a temperature of 45 °C, the hydroxyl group absorption value increased to 3298 cm^{-1} with an average absorption wavelength range of 3465-3206 cm^{-1}, showing an increase from 3269 cm^{-1} at 30 °C. Furthermore, at a temperature of 60 °C, the absorption value increased further to 3304 cm^{-1} with an average absorption wavelength range of 3455-3006 cm^{-1}. At a temperature of 75 °C, the hydroxyl absorption value decreased to 3299 cm^{-1} with an average absorption wavelength range of 3460-3151 cm^{-1}. Then, at a temperature of 90 °C, the absorption value of the hydroxyl group reached 3305 cm^{-1} with an average absorption wavelength of 3489-3011 cm^{-1} and reached its highest value. The spectral features suggest that the intermolecular interactions are predominantly governed by hydrogen bonding rather than the formation of covalent crosslinks.

Fig. 7 shows a cross-linking preparation scheme showing a PVA/TA/CNF mixture that produces a hydrogel formed from hydrogen bonds. This hydrogel is facilitated by hydroxyl groups on PVA molecules, which interact with TA and CNF hydrogel molecules to form cross-links, as shown in the cross-linking mechanism visualized in Fig. 8.

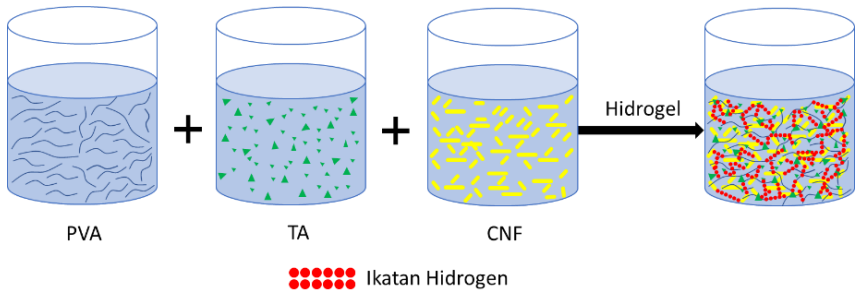

Fig. 7. Schematic illustration of the preparation of PVA/TA/CNF hydrogel cross-linking formation

Bio-based devices, especially those using PVA and TA, utilize hydroxyl groups to bind mechanical properties and efficacy. Hydroxyl groups play an important role in the formation of hydrogen bonds; they are also very important in the cross-linking process, which improves adhesive performance. PVA is a water-soluble synthetic polymer with hydroxyl groups that make it easier to interact with other molecules and form hydrogen bonds with them. This property is very important for adhesive manufacturing as it can increase adhesive strength and hydrogel stability. Previous studies have shown that PVA-based adhesives adhere well to various substrates, such as skin, because hydroxyl groups aid hydrogen bonding. Furthermore, previous research has shown that the hydroxyl groups on PVA molecules can interact with boric acid to form a three-dimensional cross-linked network with improved structural integrity [28–31]. Meanwhile, in TA, its rich hydroxyl content greatly aids the mechanical properties of PVA-based hydrogels. Incorporating TA into PVA gels results in strong hydrogel bonds and cross-links between the phenolic hydroxyl groups of TA and the hydroxyl groups of PVA [32,33]. The mixing of PVA/TA/CNF materials binds hydrogen in the resulting hydrogel, as shown in Fig. 7. The addition of CNF to the PVA-TA system has been shown to improve the mechanical properties of the resulting hydrogel. It is noted that the modification of the CNF surface with TA increases the number of polar functional groups available for hydrogen bonding with PVA, resulting in stronger interfacial adhesion and higher composite toughness [34].

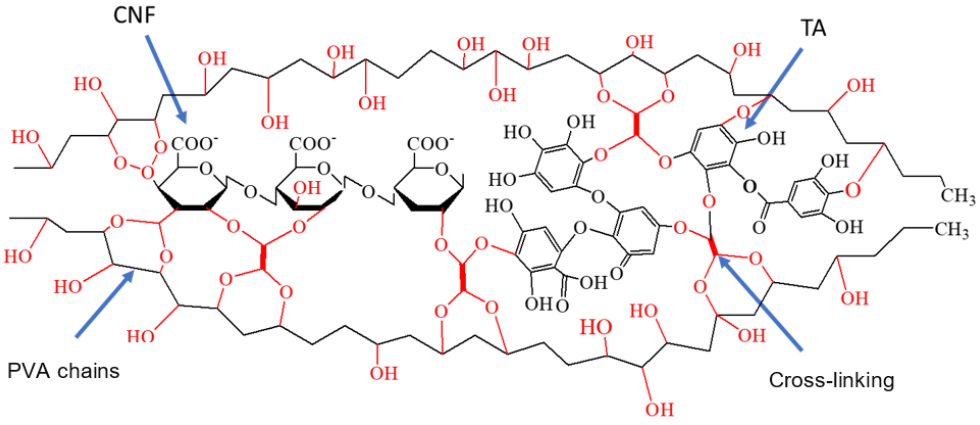

Fig. 8. Schematic illustration of PVA/TA/CNF cross-linking in hydrogel formation

The mixing of PVA/TA/CNF produces cross-links that reduce free compounds in the hydroxyl group. This can be seen in Fig. 8, which shows that extensive hydrogen bonding between the hydroxyl groups of PVA and TA results in improved bond performance and stability. The properties of PVA/TA hydrogel are enhanced by CNF. This is because the presence of CNF in the PVA-TA system results in the formation of a network structure that allows additional hydrogen bonding interactions [18,35,36], which increase the mechanical strength and toughness of the hydrogel [37]. An increase in processing temperature reduces the viscosity of the bioadhesive matrix, thereby enhancing molecular mobility and improving interfacial wetting. The lower

viscosity facilitates more effective air release during mixing, resulting in a reduction of entrapped voids and a more compact microstructure. This improved structural homogeneity promotes closer intermolecular contact among functional groups, thereby increasing the probability of hydrogen bond formation. Consequently, the enhanced hydrogen bonding interactions contribute to the observed improvement in shear strength. Overall, the enhanced hydrogen-bonding network formed by the synergistic interaction of PVA, TA, and CNF in increasing of temperature significantly improves the mechanical integrity and adhesion performance, demonstrating the suitability of the PVA/TA/CNF for bioadhesive applications.

4. Conclusions

This study shows that the PVA/TA/CNF bioadhesive achieved optimal performance at 90 °C, reaching a maximum shear strength of 3.41 MPa. At this temperature, microstructural analysis indicated significant void reduction, while FTIR revealed a hydroxyl absorption band at 3305 cm^{-1}, suggesting enhanced hydrogen-bond-based intermolecular interactions. These findings establish a temperature–structure–property relationship in which increased temperature reduces viscosity, minimizes voids, promotes intermolecular contact, and ultimately improves shear strength. Practically, 90 °C represents an effective processing window under the investigated conditions. However, the study is limited to a single composition and relies on indirect spectroscopic evidence. Future work should examine broader formulations and incorporate complementary characterization techniques to further validate the interaction mechanisms and optimize processing parameters. Although optimal performance was achieved at 90 °C, further investigation into long-term durability, moisture resistance, and substrate variability is required to assess industrial applicability.

Data availability statement

Data will be made available on request.

CRediT authorship contribution statement

Mastariyanto Perdana: Writing – original draft, Visualization, Software, Investigation. **Hairul Abral**: Supervision, Resources, Methodology, Funding acquisition, Conceptualization. **Lovely Son**: Supervision, Methodology, Review & editing. **Nanang Masruchin**: Supervision, Resources, Data curation. **Muhammad Azmi**: Investigation, Software. **Kadriadi**: Investigation, Editing.

Declaration of Competing Interest

The authors declare that they have no known competing financial interests or personal relationships that could have appeared to influence the work reported in this paper.

Acknowledgement

The authors are grateful to the Directorate General of Research, Technology and Higher Education, Indonesia, for the financial support of this research with grant number of 72/UN16.19/PT.01.03/2023. The authors would like to express their sincere gratitude to the Nanoscience and Technology Laboratory, Universitas Andalas and the Materials Laboratory-Mechanical Engineering Department, Institut Teknologi Padang, for providing facilities, technical support, and valuable assistance during the experimental work. The authors also gratefully acknowledge the support of the laboratory facilities at the National Research and Innovation Agency (BRIN) for instrumentation access and characterization support that significantly contributed to this research.

References

[1] Hasan Faris A. Fillers in Wood Adhesives. Fillers, IntechOpen; 2021. https://doi.org/10.5772/intechopen.92150.

[2] Song S, Drotlef D-M, Majidi C, Sitti M. Controllable load sharing for soft adhesive interfaces on three-dimensional surfaces. Proceedings of the National Academy of Sciences 2017;114. https://doi.org/10.1073/pnas.1620344114.

[3] Kaczmarek-Szczepańska B, Sosik A, Małkowska A, Zasada L, Michalska-Sionkowska M. The Study of Physicochemical Properties and Blood Compatibility of Sodium Alginate-Based Materials via Tannic Acid Addition. Materials 2021;14:4905. https://doi.org/10.3390/ma14174905.

[4] Yang Z, Bai T, Li T, Sha X, Ji X, Yang Y, et al. Dense H-Bonding Enhanced Bio-Based Supramolecular Adhesive: High Adhesive Strength and Multi-Reusability. ACS Appl Polym Mater 2024;6:8142–9. https://doi.org/10.1021/acsapm.4c01028.

[5] Rahim MdA, Centurion F, Han J, Abbasi R, Mayyas M, Sun J, et al. Polyphenol-Induced Adhesive Liquid Metal Inks for Substrate-Independent Direct Pen Writing. Adv Funct Mater 2021;31. https://doi.org/10.1002/adfm.202007336.

[6] Qie R, Zajforoushan Moghaddam S, Thormann E. Fully Biobased Adhesive from Chitosan and Tannic Acid with High Water Resistance. ACS Sustain Chem Eng 2024;12:4456–63. https://doi.org/10.1021/acssuschemeng.3c07306.

[7] Schmidt G, Christ PE, Kertes PE, Fisher R V., Miles LJ, Wilker JJ. Underwater Bonding with a Biobased Adhesive from Tannic Acid and Zein Protein. ACS Appl Mater Interfaces 2023;15:32863–74. https://doi.org/10.1021/acsami.3c04009.

[8] Jailani A, Ahmed B, Lee J-H, Lee J. Inhibition of Agrobacterium tumefaciens Growth and Biofilm Formation by Tannic Acid. Biomedicines 2022;10:1619. https://doi.org/10.3390/biomedicines10071619.

[9] Bu K-B, Kim M, Sung J-S, Kadam AA. Halloysite Nanotubes Decorated with Fe_3O_4 Nanoparticles and Tannic Acid for Effective Inhibition of *E. coli* Biofilm. ACS Appl Nano Mater 2024;7:313–22. https://doi.org/10.1021/acsanm.3c04518.

[10] Balanikas E, Banyasz A, Baldacchino G, Markovitsi D. Guanine Radicals Generated in Telomeric G-Quadruplexes by Direct Absorption of Low-Energy UV Photons: Effect of Potassium Ions. Molecules 2020;25:2094. https://doi.org/10.3390/molecules25092094.

[11] Zhou W, Yuan Z, Li G, Ouyang J, Suo Y, Wang H. Isolation and structure determination of a new flavone glycoside from seed residues of seabuckthorn (*Hippophae rhamnoides* L.). Nat Prod Res 2018;32:892–7. https://doi.org/10.1080/14786419.2017.1366481.

[12] He M. Tannic Acid-Based Antimicrobial Coatings. Mechanisms and Applications Frontiers in Bioengineering and Biotechnology 2022;10. https://doi.org/10.3389/fbioe.2022.981504.
[13] Li B, Whalen JJ, Humayun MS, Thompson ME. Reversible Bioadhesives Using Tannic Acid Primed Thermally-Responsive Polymers. Adv Funct Mater 2020;30. https://doi.org/10.1002/adfm.201907478.
[14] Schmidt G, Smith KH, Miles LJ, Gettelfinger CK, Hawthorne JA, Fruzyna EC, et al. Tunable Tannic Acid–Zein Adhesives for Bonding Different Substrates. Adv Sustain Syst 2022;6. https://doi.org/10.1002/adsu.202100392.
[15] Din Z, Chen L, Xiong H, Wang Z, Ullah I, Lei W, et al. Starch: An Undisputed Potential Candidate and Sustainable Resource for the Development of Wood Adhesive. Starch - Stärke 2020;72. https://doi.org/10.1002/star.201900276.
[16] Yuan X, Bian R, Lyu Y, Li C, Li X, Luo J, et al. Preparation of tannic acid-based recyclable adhesive with high adhesion property, low curing temperature, and environmental tolerance. Ind Crops Prod 2024;222:119997. https://doi.org/10.1016/j.indcrop.2024.119997.
[17] Gavrilović-Grmuša I, Rančić M, Tešić T, Stupar S, Milošević M, Gržetić J. Bio-Epoxy Resins Based on Lignin and Tannic Acids as Wood Adhesives—Characterization and Bonding Properties. Polymers (Basel) 2024;16:2602. https://doi.org/10.3390/polym16182602.
[18] Perdana M, Son L, Abral H, Masruchin N, Azmi M, Rahmadiawan D. Proceedings of the 4th South East Asia-Japan Conference on Composite Materials. vol. 82. Singapore: Springer Nature Singapore; 2025. https://doi.org/10.1007/978-981-96-8578-3.
[19] ASTM Standard 1002. Test Method for Apparent Shear Strength of Single-Lap-Joint Adhesively Bonded Metal Specimens by Tension Loading (Metal-to-Metal) 2019. https://doi.org/10.1520/D1002-10R19.
[20] Wulan N, Fajri M, sari. Analisis Fitokimia dan Gugus Fungsi dari Ekstrak Etanol Pisang Goroho Merah (Musa Acuminate (L)). IJOBB (Indonesian Journal of Biotechnology and Biodiversity) 2018;30:2. https://doi.org/10.47007/ijobb.v2i1.
[21] Sutikno E. Analisisi Tegangan Akibat Pembebanan Statis pada Desain Carbody TeC Railbus Dengan Metode Elemen Hingga'. Jurnal Rekayasa Mesin 2011;2:65–81. https://doi.org/10.21776/jrm.v2i1.127.
[22] Hossain MK, Chowdhury MMR, Salam MB, Malone J, Hosur M V., Jeelani S, et al. Improved thermomechanical properties of carbon fiber reinforced epoxy composite using amino functionalized XDCNT. J Appl Polym Sci 2014;131. https://doi.org/10.1002/app.40709.
[23] Reddy L, S, Rao NV, R, Rao TD, G. Shear Response of Fibrous High Strength Concrete Beams without Web Reinforcement. Civil Engineering Dimension 2011;13. https://doi.org/10.9744/ced.13.1.50-58.
[24] Saadatyar S, Beheshty MH, Sahraeian R. Mechanical properties of multiwall carbon nanotubes/unidirectional carbon fiber-reinforced epoxy hybrid nanocomposites in transverse and longitudinal fiber directions. Polymers and Polymer Composites 2021;29:S74–84. https://doi.org/10.1177/0967391120986516.
[25] Costa ML, Rezende MC, De Almeida SFM. Strength of Hygrothermally Conditioned Polymer Composites with Voids. J Compos Mater 2005;39:1943–61. https://doi.org/10.1177/0021998305051807.
[26] Ma W, Liu F. EFFECTS OF POROSITY ON ULTRASONIC CHARACTERISTIC PARAMETERS AND MECHANICAL PROPERTIES OF GLASS FIBER REINFORCED COMPOSITES. Int J Mod Phys Conf Ser 2012;06:646–51. https://doi.org/10.1142/S2010194512003911.
[27] Luo L, Zhang B, Lei Y, Zhang G, Zhang Z, Meng B, et al. Identification of voids and interlaminar shear strengths of polymer-matrix composites by optical microscopy

experiment and deep learning methodology. Polym Adv Technol 2021;32:1853–65. https://doi.org/10.1002/pat.5226.

[28] Zhang Y, Hui B, Ye L. Preparation and Structure of Poly(vinyl alcohol)/Polyacrylate Elastomer Composite Hydrogels and Their Application in Wastewater Treatment by Immobilizing with Microorganisms. Ind Eng Chem Res 2016;55:9934–43. https://doi.org/10.1021/acs.iecr.6b02313.

[29] Chen M, Wu Y, Chen B, Tucker AM, Jagota A, Yang S. Fast, strong, and reversible adhesives with dynamic covalent bonds for potential use in wound dressing. Proceedings of the National Academy of Sciences 2022;119. https://doi.org/10.1073/pnas.2203074119.

[30] Yu H, Xia Y, Jin Z, Zhang L, Liu X, Chen H, et al. The analysis of response surface optimization and performance of cross-linked starch/tannic acid adhesive reinforced by phragmites fibers. Polym Compos 2024;45:7495–506. https://doi.org/10.1002/pc.28281.

[31] Rahmadiawan D, Abral H, Railis RM, Iby IC, Mahardika M, Handayani D, et al. The Enhanced Moisture Absorption and Tensile Strength of PVA/Uncaria gambir Extract by Boric Acid as a Highly Moisture-Resistant, Anti-UV, and Strong Film for Food Packaging Applications. Journal of Composites Science 2022;6:337. https://doi.org/10.3390/jcs6110337.

[32] Si C, Tian X, Wang Y, Wang Z, Wang X, Lv D, et al. A Polyvinyl Alcohol–Tannic Acid Gel with Exceptional Mechanical Properties and Ultraviolet Resistance. Gels 2022;8:751. https://doi.org/10.3390/gels8110751.

[33] Jackson J, Dietrich CH. Synergistic Antibacterial Effects of Gallate Containing Compounds with Silver Nanoparticles in Gallate Crossed Linked PVA Hydrogel Films. Antibiotics 2024;13:312. https://doi.org/10.3390/antibiotics13040312.

[34] Liu J, Huang H, Zhou D. Surface modification of cellulose nanofibers by oxidative polymerization of tannic acid/ethanediamine and their polyvinylalcohol composites. J Appl Polym Sci 2022;139. https://doi.org/10.1002/app.53049.

[35] Abral H, Kurniawan A, Rahmadiawan D, Handayani D, Sugiarti E, Muslimin AN. Highly antimicrobial and strong cellulose-based biocomposite film prepared with bacterial cellulose powders, Uncaria gambir, and ultrasonication treatment. Int J Biol Macromol 2022;208:88–96. https://doi.org/10.1016/j.ijbiomac.2022.02.154.

[36] Sawant M, Chakraborty T, Yadav D, Biranje S, Saxena S, Shukla S. Stabilization strategies and optimization of polyvinyl alcohol-chitosan hybrid polymer. Hybrid Advances 2025;8:100345. https://doi.org/10.1016/j.hybadv.2024.100345.

[37] Tan R, Li F, Zhang Y, Yuan Z, Feng X, Zhang W, et al. High-Performance Biocomposite Polyvinyl Alcohol (PVA) Films Modified with Cellulose Nanocrystals (CNCs), Tannic Acid (TA), and Chitosan (CS) for Food Packaging. J Nanomater 2021;2021:1–9. https://doi.org/10.1155/2021/4821717.